

# THE MULTIPACTING STUDY OF NIOBIUM SPUTTERED HIGH-BETA QUARTER-WAVE RESONATORS FOR HIE-ISOLDE

P. Zhang\* and W. Venturini Delsolaro  
CERN, Geneva, Switzerland

## Abstract

Superconducting Quarter-Wave Resonators (QWRs) will be used in the superconducting linac upgrade in the frame of HIE-ISOLDE project at CERN. The cavities are made of bulk copper with thin niobium film coated. They will be operated at 101.28 MHz at 4.5 K providing 6 MV/m accelerating gradient with 10 W maximum power dissipation. Multipacting (MP) has been studied for the high-beta ( $\beta=10.9\%$ ) QWRs and two MP barriers have been found:  $E_{acc}$  at around 0.05 MV/m and 1.5 MV/m. We have used both CST Microwave Studio & Particle Studio and the parallel codes Omega3P & Track3P developed at SLAC. The results from the two codes are consistent and are in good agreement with cavity vertical cold test results. Both MP barriers can be conditioned by RF processing.

## INTRODUCTION

The ISOLDE project at CERN is under a major upgrade to boost both the energy and intensity of the radioactive beam [1]. This includes replacing part of the existing normal conducting linac with superconducting quarter-wave resonators (QWRs). The QWRs are made of bulk copper (Cu) coated with thin niobium (Nb) film [2]. They will be operated with a frequency of 101.28 MHz at 4.5 K. Each QWR will provide an accelerating gradient of 6 MV/m on beam axis with a maximum of 10 W power dissipation on the cavity inner surface. Two types of QWRs, low- $\beta$  (6.3%) and high- $\beta$  (10.3%), are planned to be installed in 3 phases to cover the entire energy range [1]. Since the linac upgrade started from the high energy section, all R&D efforts have been focussed on the high- $\beta$  QWRs [3]. A CAD model of the cavity is shown in Fig. 1(a) and its main RF parameters are listed in Table 1.

The electromagnetic field distribution in the cavity simulated with CST Microwave Studio® [4] is shown in Fig. 1(b)(c). The peak electric field is at the tip of the inner conductor and can go up to 30 MV/m during normal operation. The magnetic field, on the other hand, peaks at the top part of the cavity and can reach 57 mT when  $E_{acc}=6$  MV/m.

Cavity RF cold tests have shown multipacting (MP) at various field levels requiring dedicated processing time. Therefore MP simulations have been carried out in order to improve the understanding of this phenomena in these

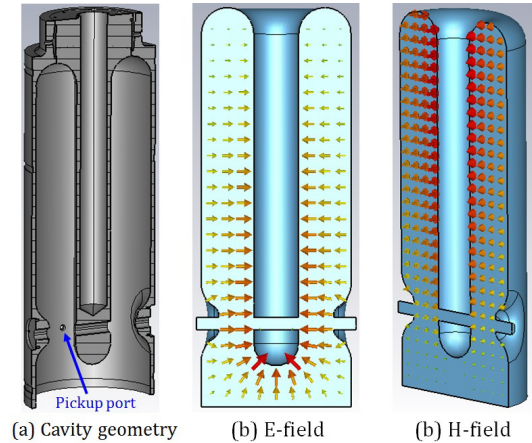


Figure 1: The cavity geometry and its electromagnetic field distribution simulated using CST Microwave Studios®.

Table 1: The main RF Parameters of the High- $\beta$  QWR

Parameter	Value
$f_0$ at 4.5 K [MHz]	101.28
$\beta_{optimum}$ [%]	10.9
$E_{peak}/E_{acc}$	5.0
$B_{peak}/E_{acc}$ [mT/(MV/m)]	9.5
geometry factor $G=R_s Q_0$ [ $\Omega$ ]	30.8
nominal gradient $E_{acc}$ [MV/m]	6
max power dissipation at 6 MV/m [W]	10
$Q_0$ at $E_{acc}=6$ MV/m	$4.7 \times 10^8$

cavities. The simulations are in good agreement with results from cavity RF cold tests.

## MULTIPACTING STUDIES BY SIMULATIONS

Two sets of codes have been used to study the MP phenomena: CST Microwave Studio® & Particle Studio® [4] and SLAC Omega3P & Track3P [5]. These will be described in the following sections.

### Multipacting Study by CST Code Suite

A typical secondary electron yield (SEY) curve for Nb is shown in Fig. 2. The SEY is greater than 1 when the energy of the electron impacting on the Nb surface falls into

\*pei.zhang@cern.ch

80–2000 eV range. The resonant particles with impact energy residing in this range will likely lead to MP. The MP studies were carried out in two steps: The electromagnetic (EM) field was first simulated by CST Microwave Studio (Fig. 1(b)(c)) using the eigenmode solver, and then the MP simulation was done by CST Particle Studio with Tracking solver using the already simulated EM field. The SEY curve shown in Fig. 2 is used for the inner surface of the Nb-coated cavity.

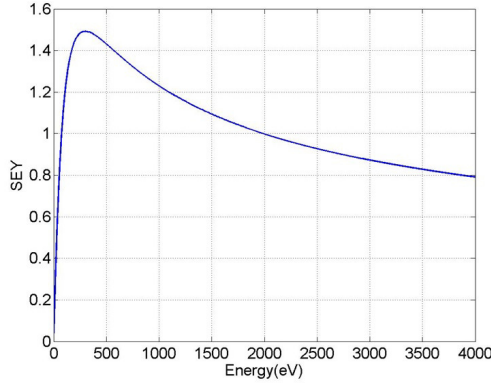


Figure 2: The SEY curve of niobium after 300°C bake [4].

In order to reduce the computation load and for the ease of analysis, the cavity inner surface has been partitioned into several regions at top part, upper part and lower part. Particles were emitted on the faces of each region with an initial energy of 2 eV. Then the spatial position and energy of the particles are tracked under the influence of EM field inside the cavity. The space charge effect was ignored. Both the magnitude and the phase of the cavity field were varied, and tracking was done for each field magnitude and phase combination. The accelerating field level was scanned up to 6 MV/m with a RF phase scan interval of 30° for each field level.

The particle trajectories on the top part of the cavity are shown in Fig. 3 after certain number of RF cycles. One can see that considerable amount of particles are generated after only 10 RF cycles (~100 ns). This is clearly shown in the plot of number of particles inside the cavity with time. An evident exponential growth of particle number with time can be seen. In addition, most of the resonant particles survived after 10 RF cycles have the energy below 2 keV. This is supported by the larger SEY value within this energy range as shown in Fig. 2. The corresponding accelerating field level in the cavity is 1.5 MV/m with a phase of 330° with regarding to the launching of the initial particles.

At the lower part of the cavity, the particles can also build up resonance but at rather low field level (Eacc~0.05 MV/m). As shown in Fig. 4, the exponential growth becomes evident after 4 RF cycles. Similar MP behaviour is also observed on the upper part of the cavity as shown in Fig. 5. In both cases, the particle energy remains low (<3 keV).

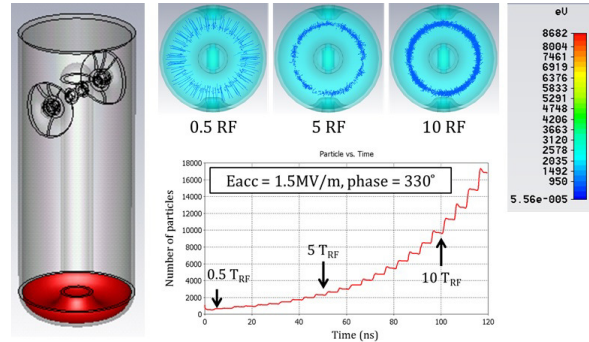


Figure 3: The MP on cavity top part simulated with CST.

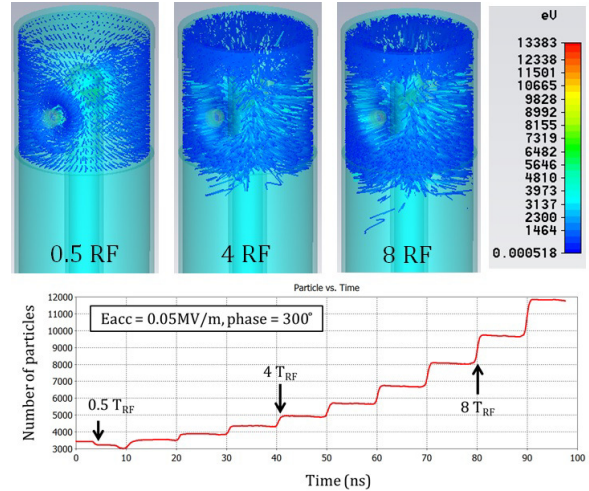


Figure 4: The MP on cavity lower part simulated with CST.

In order to evaluate the MP probability, the normalized secondary electron yield is calculated as [6]

$$\langle SEY \rangle = \frac{I_{SEE}}{I}, \quad (1)$$

where  $I_{SEE}$  is the emitted current from the impact surface due to secondary electrons, and  $I$  is the current observed by the impact surface due to particle collisions. In this way,  $\langle SEY \rangle$  is a measure of the magnitude of MP. The  $\langle SEY \rangle$  has been calculated for each field level for all regions. As shown in Fig. 6, two MP barriers are found at Eacc ~1.2 MV/m and ~0.05 MV/m. The high-field MP barrier is located at the top part of the cavity while the low-field barrier is on the cavity body.

### Multipacting Study by ACE3P Code Suite

The EM simulation was done by using Omega3P and the electromagnetic field profile is shown in Fig. 7(b)(c). Subsequently Track3P was used to track particles and identify resonant trajectories. The cavity was also partitioned but into only two regions as shown in Fig. 7(a) for the ease of simulation and analysis.

Two MP barriers were found at Eacc ~1.4 MV/m and ~0.05 MV/m. The high-field MP occurs at the top part

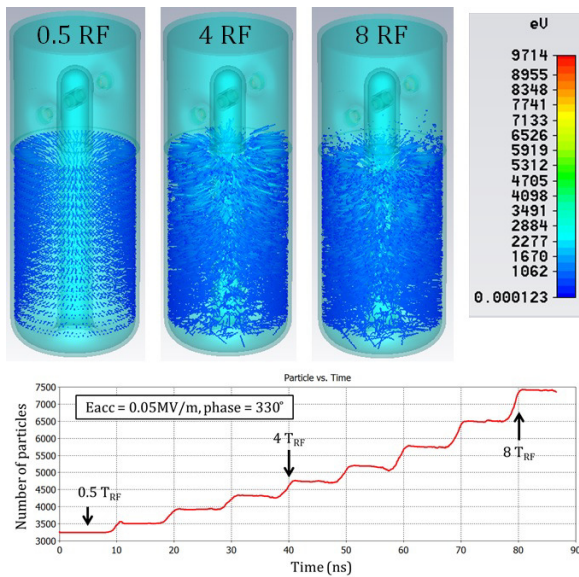


Figure 5: The MP on cavity upper part simulated with CST.

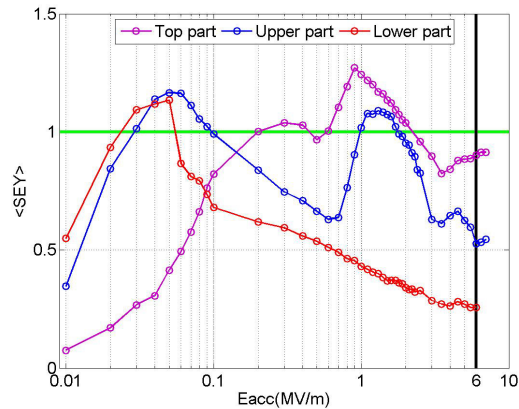


Figure 6: The normalized SEY calculated from CST simulation results.

of the cavity. The trajectory of one particle is shown in Fig. 8(b). After a few RF cycles, the particle moves to the very top of the cavity and it turns out to be a two-point MP oscillating around the top welding. This can be seen from the final particle impact position shown in Fig. 8(a). The impact energy of resonant electrons at this region is shown in Fig.8(c). Knowing that the SEY of Nb is greater than 1 above 80 eV, the MP band in this region is  $E_{acc}=1.4\text{--}1.6$  MV/m.

The low-field MP barrier is at the cavity body as shown in Fig. 9(a) and Fig. 10(a). The impact energy of the electrons shown in Fig. 9(b) and Fig. 10(b) indicate a MP band of  $E_{acc}=0.02\text{--}0.08$  MV/m.

ISBN 978-3-95450-178-6

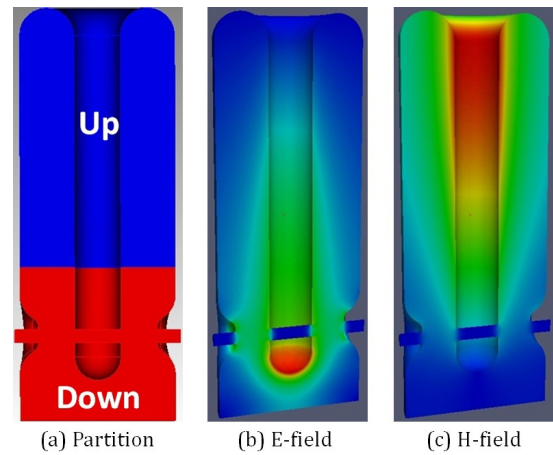


Figure 7: The partition of the cavity geometry (a) and the simulated EM field (b)(c).

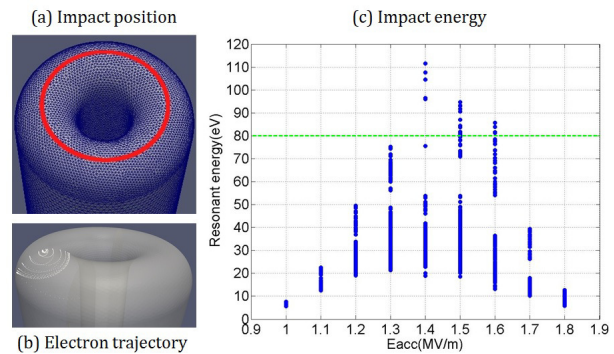


Figure 8: (a) The impact position of resonant particles after 40 RF periods. (b) The trajectory of one resonant electron. (c) The impact energy vs. accelerating gradient for particles with resonant trajectories on the top part of the cavity.

### EXPERIMENTAL RESULTS FROM RF COLD TESTS

The cavity quality factor  $Q_0$  of 10 different high- $\beta$  QWRs have been recorded during 14 vertical tests at 4.5 K when MP occurred as shown in Fig. 11. Two MP barriers are clearly visible at  $E_{acc}\sim 0.05$  MV/m and  $\sim 1.5$  MV/m. The  $E_{acc}$  value when MP starts is shown in Fig. 12. These are very consistent with simulation results from both codes. In particular, Fig. 12(b) resembles Fig. 8(c). The low statistics for the low-field MP measurements is due to lack of occurrence at 4.5 K after successful warm RF conditioning.

The warm RF conditioning for MP normally started when the cavity is at about 200 K with the surrounding thermal shield at 60 K. At that time, the cavity remains in its normal conducting state and the cavity  $Q_0$  is  $\sim 10^4$ . Each QWR is equipped with a mobile coupler whose  $Q_{ext}$  can be varied from  $10^4$  to  $10^{11}$  [7]. During the warm conditioning, the coupler was fully inserted into the cavity to match as much as possible to the  $Q_0$ . It normally gives a coupling

SRF Technology - Cavity

E07-Non-Elliptical performance

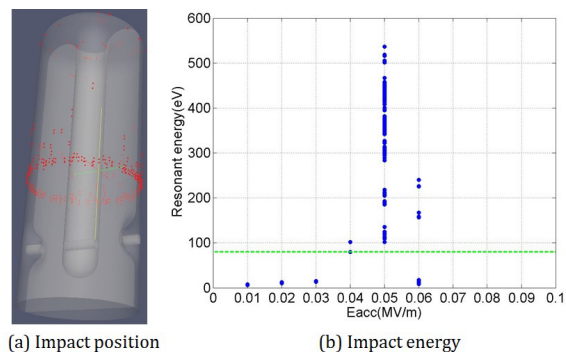


Figure 9: (a) The impact position of resonant particles after 40 RF periods. (b) The impact energy vs. accelerating gradient for particles with resonant trajectories on the upper part of the cavity.

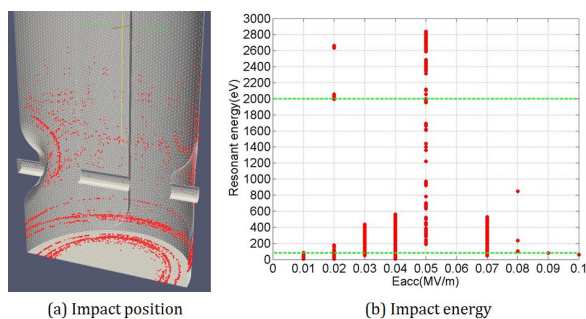


Figure 10: (a) The impact position of resonant particles after 40 RF periods. (b) The impact energy vs. accelerating gradient for particles with resonant trajectories on the lower part of the cavity.

factor  $\beta$  of  $\sim 0.6$ . In this case, a forward power of  $\sim 50$  W is sufficient to raise the cavity field to 0.05 MV/m at normal conducting state. Thus the low-field MP can be fully conditioned before the cavity becomes superconducting. However, a much higher forward power ( $\sim 45$  kW) would be required to reach the high-field MP barrier at  $\sim 1.5$  MV/m at normal conducting state. This is not feasible with our current setup for the cold test. Therefore the warm conditioning is only to process the low-field MP barrier while the high-field MP is processed at 4.5 K. There are two advantages for warm conditioning: firstly, the cavity is easy to be locked to the driving RF due to relatively large loaded bandwidth ( $\sim$ kHz), thus drastically reduced the MP conditioning time if otherwise done at 4.5 K; Secondly, most MP conditioning was conducted during the cavity cooldown, which saves some processing time at 4.5 K (a few hours).

The pickup antenna is located at the lower part of the cavity as shown in Fig. 1(a). A typical spectrum measured from the pickup antenna when the cavity falls into the low-field MP band is shown in Fig. 13. One can clearly see side bands around the fundamental mode, and this is caused by the activities of the MP electrons inside the cavity. The spacing and the shape of the side bands vary with the for-

SRF Technology - Cavity

E07-Non-Elliptical performance

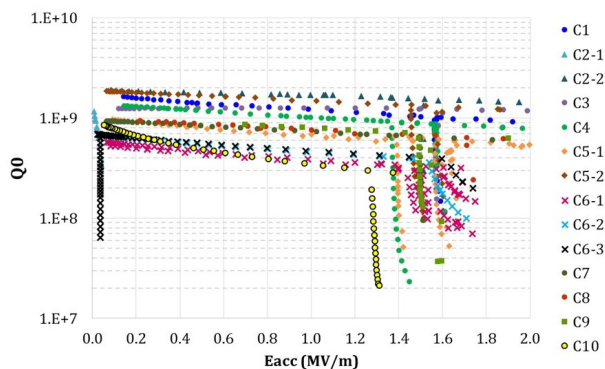


Figure 11: The Q vs. Eacc curves measured in 14 RF cold tests on 10 different cavities.

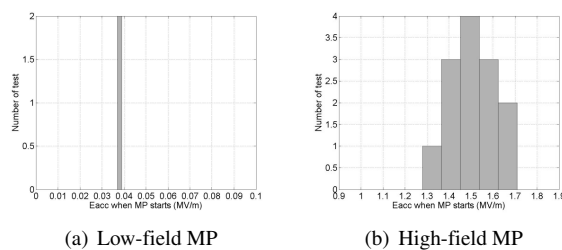


Figure 12: The measured Eacc when MP starts.

ward power in other words the cavity field strength. On the other hand, no side bands was observed in the high-field MP barrier ( $\sim 1.5$  MV/m) since the location of the electron resonance is on the cavity top part as shown in Fig. 3 and Fig. 8. This is far from the pickup location.

In our previous cavity cold tests, the warm conditioning takes only a few hours to pass the low-field MP barrier and the cavity subsequently starts clean from low-field at 4.5 K. On the other hand, the high-field MP barrier turned out to be very soft for almost all cavities and it takes from a few minutes to 1 hour to process.

### FINAL REMARKS

CST Particle Studio and SLAC Track3P were used to analyze the MP barriers in the HIE-ISOLDE high- $\beta$  QWRs. Two MP bands were found:  $E_{acc}=0.02-0.08$  MV/m and  $\sim 1.5$  MV/m. These are in well agreement with cavity vertical test results. Both barriers are not persistent and can be processed by RF conditioning.

### ACKNOWLEDGEMENTS

We thank M. Therasse, S. Bizzaglia, S. Fiotakis, M. Gourragne, G. Pechaud and G. Fernandez for their help in preparing the cold measurements. We are grateful to R. Torres-Sanchez and G. Burt for very enlightening discussions. We also thank A. Miyazaki for providing the cold test measurement data of one cavity. This work has been supported partly by a Marie Curie Early

ISBN 978-3-95450-178-6

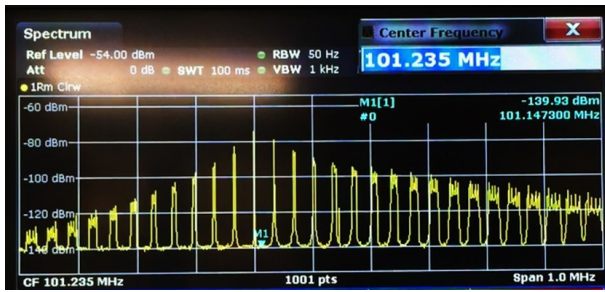


Figure 13: The spectrum measured from the cavity pickup antenna during MP conditioning above 10K.

Initial Training Network Fellowship of the European Community's 7th Programme under contract number PITN-GA-2010-264330-CATHI.

## REFERENCES

- [1] W. Venturini Delsolaro *et al.*, "Status of the HIE Isolde Project including Cryomodule Commissioning," in *these proceedings*, 2015.
- [2] A. Sublet *et al.*, "Nb Coated HIE-ISOLDE QWR Superconducting Accelerating Cavities: From Process Development to Series Production," in *Proceedings of IPAC2014*, 2014.
- [3] P. Zhang *et al.*, "The tuning system for HIE-ISOLDE high-beta quarter-wave resonators," in *Proceedings of SRF2013*, 2013.
- [4] CST Microwave Studio®. Ver. 2013, CST AG, Darmstadt, Germany.
- [5] C.-K. Ng *et al.*, "Advances in Parallel Finite Element Code Suite ACE3P," in *Proceedings of IPAC2015*, 2015.
- [6] G. Burt *et al.*, "Prediction of multipactor in the iris region of rf deflecting mode cavities," *Phys. Rev. ST Accel. Beams*, vol. 14, p. 122002, 2011.
- [7] P. Zhang *et al.*, "Frequency pre-tuning of the niobium-sputtered quarter-wave resonator for HIE-ISOLDE project at CERN," *Nuclear Instruments and Methods in Physics Research Section A: Accelerators, Spectrometers, Detectors and Associated Equipment*, vol. 797, pp. 101 – 109, 2015.